Copy 265
RM E52I30

NACA

RESEARCH MEMORANDUM

FORCE AND PRESSURE-RECOVERY CHARACTERISTICS OF A CONICAL-TYPE NOSE INLET OPERATING AT MACH NUMBERS OF 1.6 TO 2.0 AND AT ANGLES OF ATTACK TO 9°

By Andrew Beke and J. L. Allen

Lewis Flight Propulsion Laboratory
Cleveland, Ohio

NATIONAL ADVISORY COMMITTEE FOR AERONAUTICS

WASHINGTON

November 19, 1952

NATIONAL ADVISORY COMMITTEE FOR AERONAUTICS

RESEARCH MEMORANDUM

FORCE AND PRESSURE-RECOVERY CHARACTERISTICS OF A CONICAL-TYPE NOSE INLET OPERATING AT MACH NUMBERS OF 1.6 TO 2.0 AND AT ANGLES OF ATTACK TO 9°

By Andrew Beke and J. L. Allen

SUMMARY

An axially symmetric spike-type nose inlet suitable for a nacelle power-plant installation was investigated in the Lewis 8- by 6-foot supersonic tunnel at Mach numbers of 1.6, 1.8, and 2.0 and at angles of attack from 0° to 9°. The inlet was designed to attain a mass-flow ratio of unity at a flight Mach number of 2.0. Force and pressure-recovery data were obtained for two subsonic diffuser area variations and are presented without detailed analysis.

Both of the configurations attained critical mass-flow ratios of unity at maximum pressure recoveries from 0.84 to 0.85 at a flight Mach number of 2.0. Stable subcritical operating ranges between mass-flow ratios from 0.87 to 1.0 were obtained at the design flight Mach number for the model with a comparatively rapid initial rate of diffusion and from 0.57 to 1.0 for the model with a constant-area section extending 2.8 inlet diameters aft of the entrance.

INTRODUCTION

Until relatively recently, most inlet investigations were concerned with the measurement of pressure-recovery and mass-flow characteristics at the inlet design flight Mach number; consequently, force data are less abundant. Therefore, as part of a general program to provide design data on the force and pressure characteristics of supersonic inlets, an axially symmetric spike-type inlet suitable for a nacelle power-plant installation has been investigated in the NACA Lewis 8- by 6-foot supersonic tunnel. The inlet was designed to attain a mass-flow ratio of unity at a flight Mach number of 2.0.

Aerodynamic and pressure-recovery characteristics of the configuration with two subsonic diffuser area variations at an angle of attack of 0° are presented for a range of mass-flow ratios at flight Mach numbers

of 1.6, 1.8, and 2.0. Angle-of-attack data are presented for one of the configurations. The data are presented without detailed analysis.

SYMBOLS

The following symbols are used in this report:

A	area
A_m	external maximum cross-sectional area
C_D	external-drag coefficient

$$C_D = \frac{D}{q_0 A_m}$$

$$= \frac{\left[\gamma p_4 M_4^2 + (p_4 - p_0)\right] A_4 \cos \alpha + (p_b - p_0) A_b \cos \alpha - \gamma p_0 M_0^2 A_0}{q_0 A_m} - C_{T-D}$$

$C_{L,e}$	external-lift coefficient, $\frac{\text{External lift}}{q_0 A_m}$
C_M	pitching-moment coefficient about base of model, $\frac{G}{q_0 A_m, l}$
C_{T-D}	thrust-minus-drag coefficient, $\frac{T-D}{q_0 A_m}$
D	drag force
G	pitching moment about base of model
L	length of subsonic diffuser, 46.875 in.
l	over-all length of model, 58.72 in.
M	Mach number
m	mass flow
$\frac{m_4}{m_0}$	mass-flow ratio, $\frac{\text{mass flow through inlet}}{\rho_0 V_0 A_1}$
P	total pressure
p	static pressure

q	dynamic pressure, $\frac{\gamma p M^2}{2}$
T	thrust, net force in flight direction determined by application of momentum theorem to air passing through model
V	velocity
x	longitudinal station
α	nominal angle of attack, deg
γ	ratio of specific heats for air
ρ	mass density of air

Subscripts:

b	base of strain gage balance
x	longitudinal station
0	free stream
1	leading edge of cowl lip
4	diffuser discharge at constant diameter section, station 46.875
$4,1$	diffuser discharge at constant diameter section (sting out), station 46.875

Pertinent areas:

A_b	area at base of balance
A_m	external maximum cross-sectional area, 0.360 sq ft
A_1	inlet capture area defined by cowl lip (measured), 0.155 sq ft
A_4	flow area at diffuser discharge, 0.289 sq ft
$A_{4,1}$	flow area at diffuser discharge (sting out), 0.338 sq ft

APPARATUS AND PROCEDURE

A schematic diagram of the nacelle-type model investigated is shown in figure 1. The configuration consisted of an external-compression single-conical shock inlet and an annular subsonic diffuser. Tip projection of the 25°-half-angle cone was selected to produce a conical shock tangent to the cowl lip at a flight Mach number of 2.0. The slope of the cowl lip was nearly alined with the local flow behind the oblique shock. Coordinates of the cowl and centerbody are presented in table I. The two plates attached to the internal side of the outer body, shown in section A-A of figure 1, were used to cover access openings.

The configuration was investigated with two subsonic diffusers which had similar area variations downstream of station 22.4. The diffusers corresponding to the dashed and solid curves, as indicated in figure 2, are hereinafter designated as inlets A and B, respectively. The longitudinal area variation shown in figure 2 is the ratio of the local flow area, based on the average normal to the annulus surfaces, and the maximum cross-sectional area at the diffuser discharge, station 46.875. Changing the area variation from inlet A to inlet B (see fig. 2) was accomplished by casting metal to the removable spike portion and by adding preshaped segments to the centerbody between the spike junction and station 22.4. All junctions or cracks were filled and the resulting centerbody was finished to a smooth surface similar to the original centerbody.

The model was sting mounted from the tunnel strut. Forces were measured by a three-component strain-gage balance located inside the centerbody. The pressure acting on the base of the balance was measured by means of a static tube. A static calibration of model and sting deflections was used in conjunction with balance normal and moment readings to determine the model angle of attack. Since the balance normal and axial links were very sensitive to inlet instability, time-force histories were used to define the onset of inlet pulsing. Visual and high-speed motion-picture schlieren observations were also made.

Mass flows are expressed as the ratio of the mass flow through the model to that of a free-stream tube defined by the capture area of the cowling. Mass flow through the inlet was computed for choking at the geometric minimum area of the control plug normal to the outer body and with the use of an average static pressure measured at the plane of survey (station 36.7). The maximum deviation among the eight static-pressure tubes (arranged in six equally spaced radial segments and at various radial distances) was less than 1 percent. Mach numbers were determined by applying the isentropic one-dimensional area-ratio relation between the plane of survey and the sonic discharge. Total-pressure recoveries were computed from the average static pressure and the Mach numbers. No correction factors have been applied to the data.

Results of a static or bench test indicated that the mass flows as computed herein were within about one percent of those obtained with a calibrated venturi and that the average pressure recoveries varied less than one percent from those obtained with a slotted averaging total-pressure rake. Similar accuracies are estimated for the data obtained at angles of attack other than 0°.

The performance data of the inlets were referred to the maximum constant-area section of the diffuser (station 46.875) from the plane of survey with the flow area (at station 46.875) increased by an amount equivalent to the cross-sectional area of the support sting and by applying isentropic one-dimensional flow relation. This procedure accounts for the thrust developed between the plane of survey and the diffuser discharge (neglecting small total-pressure losses). The diffuser-discharge Mach numbers based on the area $A_{4,1}$ correspond to the measured thrust-minus-drag coefficients inasmuch as the force acting on the base (and measured by) of the strain-gage balance is, within about 1 percent, equal to that obtained by diffusing isentropically from area A_4 to $A_{4,1}$.

The Reynolds number, based on the inlet diameter, was approximately 2.2×10^6.

RESULTS AND DISCUSSION

Performance of Inlet A

The variation of total-pressure recovery, diffuser-discharge Mach number, thrust-minus-drag coefficient, and external-drag coefficient with mass-flow ratio are presented in figure 3 for flight Mach numbers of 2.0, 1.8, and 1.6 at a nominal angle of attack of zero. The actual angle of attack varied from 0.4° at flight Mach numbers of 2.0 and 1.8 to 0.6° at a flight Mach number of 1.6; however, all data have been reduced for nominal angles of attack.

The thrust-minus-drag coefficients were obtained from the strain-gage balance readings and correspond to the net force on the model in the flight direction (sting removed) or to the net propulsive thrust coefficient of a ram-jet engine developed by heat addition without losses with a straight-pipe exit. The external drag was obtained by subtracting the measured thrust-minus-drag from the computed thrust (see SYMBOLS).

At the design Mach number of 2.0 and an angle of attack of zero, a critical mass-flow ratio of unity was attained with a maximum total-pressure recovery of about 0.85 (fig. 3(a)); the external-drag coefficient for these conditions was about 0.095 (fig. 3(b)). The attainment of a mass-flow ratio of unity was also ascertained by means of schlieren

photographs. Inasmuch as the amplitude of the axial force pulsation increased slowly with decreasing mass-flow ratio, determination of the onset of inlet instability was difficult. Data at a mass-flow ratio of 0.87 indicated a moderate pulsing amplitude compared with severe pulsing between mass-flow ratios of 0.83 to 0.71. The stable subcritical operating range of the inlet is therefore between mass-flow ratios of 1.0 and 0.87.

Angle-of-attack characteristics of inlet A are not presented since these data were found to be similar in trend and magnitude to those of inlet B.

Performance of Inlet B

The force and pressure-recovery performance obtained with inlet B is presented as a function of mass-flow ratio for flight Mach numbers of 2.0, 1.8, and 1.6 in figure 4 for a nominal angle of attack of zero and in figure 5 for a nominal angle of attack of 6°. Data for nominal angles of attack of 3° and 9° at a flight Mach number of 2.0 are also presented (fig. 6). At a nominal angle of attack of zero at a flight Mach number of 2.0, the actual angle of attack was about 0.4° and at flight Mach numbers of 1.8 and 1.6 the angle of attack was about 0.7°. The external-lift and pitching-moment coefficients for all flight Mach numbers and angles of attack investigated are presented in figure 7. The external-lift and the pitching-moment coefficients include the additive components due to mass-flow spillage. The pitching-moment coefficients are referred to the base of the model and assume that the turning of the captured mass flow occurred at the cowl lip.

At the design conditions, a critical mass-flow ratio of unity was also obtained with inlet B (see fig. 4(a)); however, the maximum pressure recovery for critical mass flow was reduced slightly to about 0.84 as compared with 0.85 obtained with inlet A. This is probably a result of the higher Mach numbers existing over a greater length of the diffuser as a consequence of the constant-area section. The minimum external-drag coefficient for inlet B was the same as for inlet A within the accuracy of measurement. The stable subcritical operating range for inlet B between mass-flow ratios of 1.00 and 0.57 at a flight Mach number of 2.0 and a nominal angle of attack of zero is substantially larger than that of inlet A. At mass-flow ratios less than 0.57, the transition of the axial-force amplitude into a region of severe oscillation occurred over a small range of mass-flow ratios as compared with inlet A. The relatively constant-area section aft of the inlet entrance may have stabilized disturbances such as those generated by shock boundary-layer interaction or by the intersection of the conical and normal shocks (such as the vortex sheet mentioned in reference 1). However, the reason for the increase in the stable subcritical operating range is not hereby definitely ascertained from this singular result. Furthermore, the following minor differences in the two models restrict the generality of the preceding result:

(a) The small knob or shoulder formed by the intersection of the cone and centerbody was reduced for inlet B (see table I). This moved the extremity of the conical portion of the centerbody from a station slightly inside the cowl (0.1 in.) to a station slightly outside the cowl (-0.2 in.).

(b) The exactness of surface finish could not be duplicated for the centerbody of inlet B.

SUMMARY OF RESULTS

The following results were obtained from an investigation of the force and pressure-recovery characteristics of a conical-type nose inlet.

Both of the models investigated attained critical mass-flow ratios of unity at total-pressure recoveries between 0.84 and 0.85 at a flight Mach number of 2.0 and an angle of attack of zero. The model which had a practically constant-area section extending 2.8 inlet diameters aft of the entrance had a stable subcritical range for mass-flow ratios from unity to 0.57 compared with a range between unity and 0.87 for the model with a more rapid initial rate of diffusion.

Lewis Flight Propulsion Laboratory
National Advisory Committee for Aeronautics
Cleveland, Ohio

REFERENCE

1. Ferri, Antonio, and Nucci, Louis M.: The Origin of Aerodynamic Instability of Supersonic Inlets at Subcritical Conditions. NACA RM L50K30, 1951.

TABLE I - COORDINATES

Centerbody			Cowling		
Station (in.)	Radius (in.)		Station (in.)	External radius (in.)	Internal radius (in.)
	Inlet A	Inlet B			
-2.86	[a]0	[a]0	0.0	2.671	2.671
-.2	[a]1.24	[a]1.24	.015	2.686	2.656
.0	[a]1.32	1.32	.5	2.79	2.73
.1	[a]1.40	1.36	1.0	2.89	2.80
.2	1.42	1.39	1.5	2.97	2.86
.3	1.44	1.42	2.0	3.04	2.92
.4	1.46	1.45	2.5	3.11	2.98
.5	1.48	1.48	3.0	3.16	3.03
.8	1.54	1.56	4.0	3.25	3.12
1.0	1.58	1.61	5.0	3.32	3.20
1.5	1.67	1.73	6.0	3.38	3.25
2.0	1.74	1.84	7.0	3.42	3.30
2.5	1.81	1.92	8.0	3.45	3.33
3.0	1.88	2.01	8.67	3.47	3.35
4.0	1.99	2.14			
5.0	2.10	2.24			
6.0	2.19	2.31			
7.0	2.26	2.37			
8.0	2.30	2.42			
9.0	2.30	2.44			
10.0	2.29	2.46			
12.0	2.27	2.46			
14.0	2.24	2.44			
16.0	2.20	2.40			
18.0	2.16	2.32			
20.0	2.11	2.19			
22.4	2.03	2.03			
24.0	1.95	1.95			
28.0	1.75	1.75			
32.0	1.61	1.61			
37.1	1.50	1.50			
46.87	1.50	1.50			

[a]Region of 25°-half-angle cone.

2706

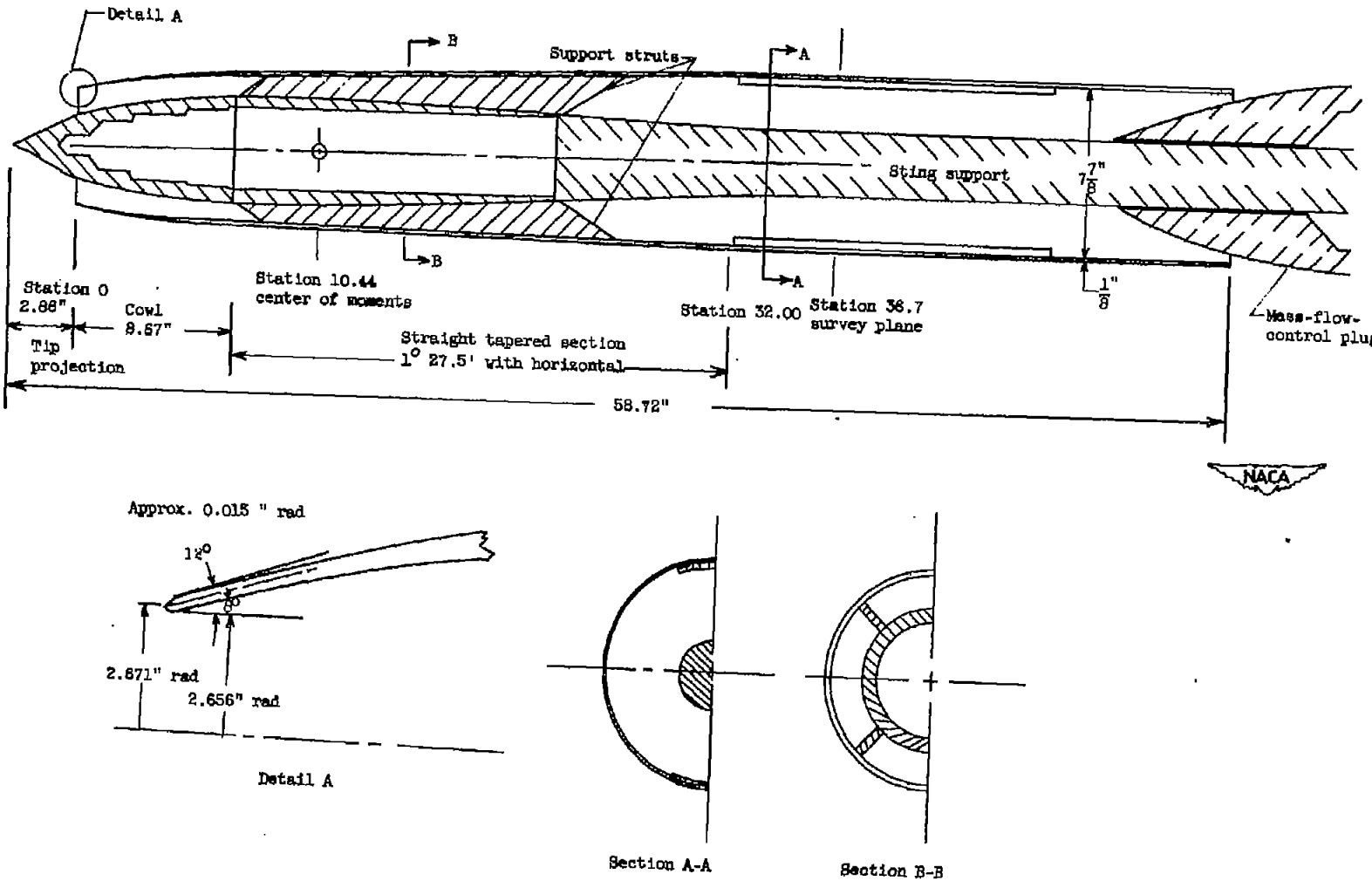

Figure 1. - Schematic diagram showing principal dimensions of model.

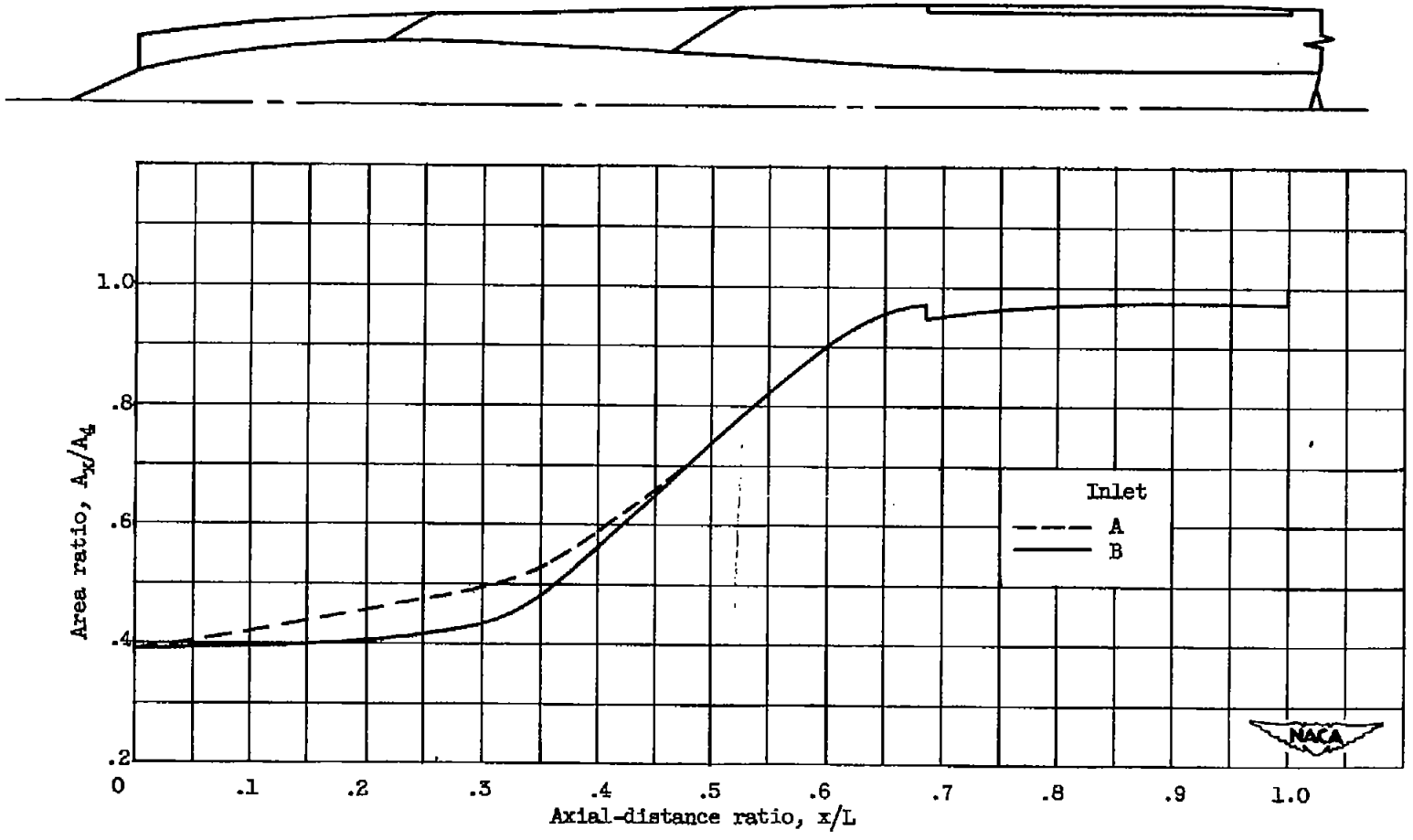

Figure 2. - Subsonic-diffuser area variation.

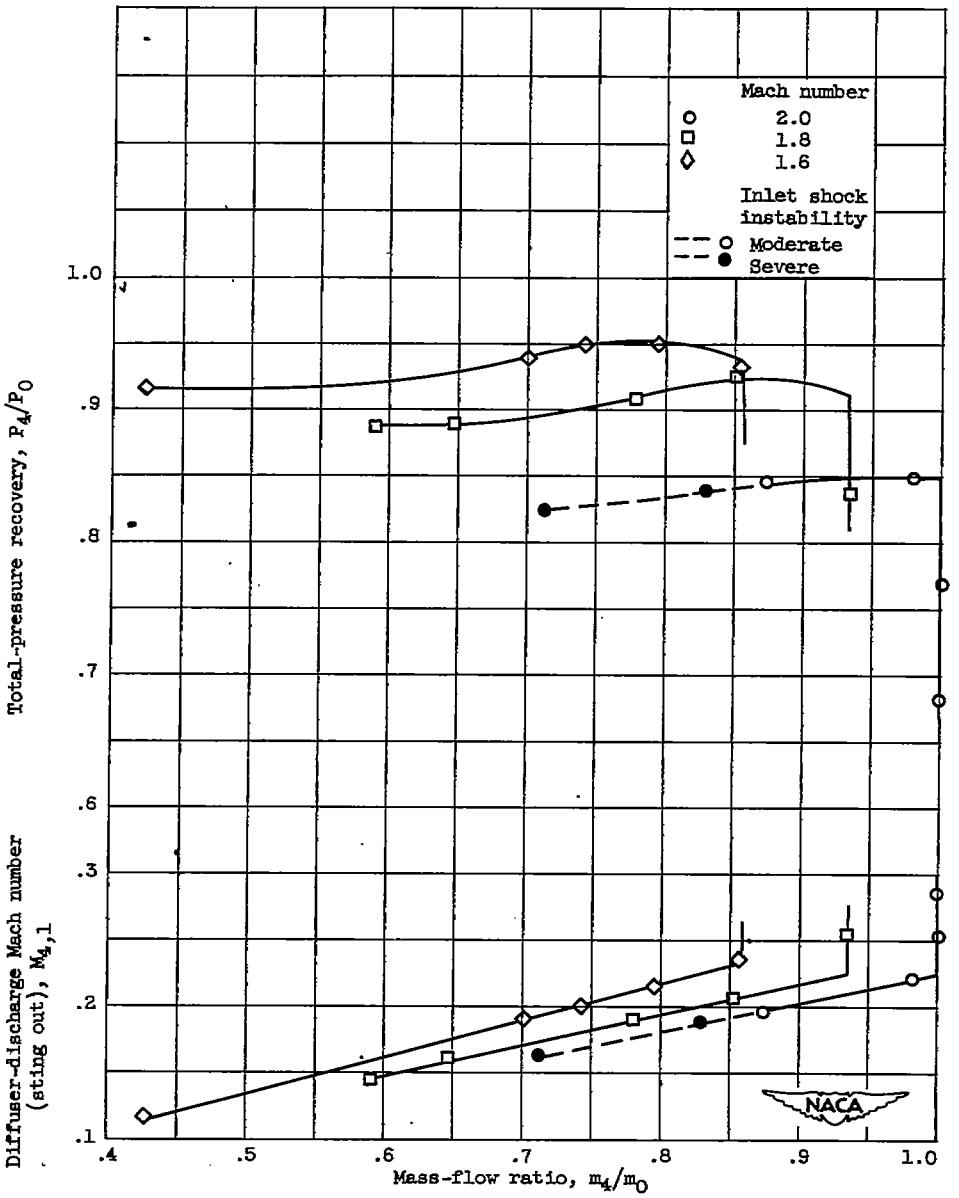

(a) Pressure-recovery and diffuser-discharge Mach number characteristics

Figure 3. - Variation of inlet characteristics with mass-flow ratio for range of Mach numbers. Inlet A at zero angle of attack.

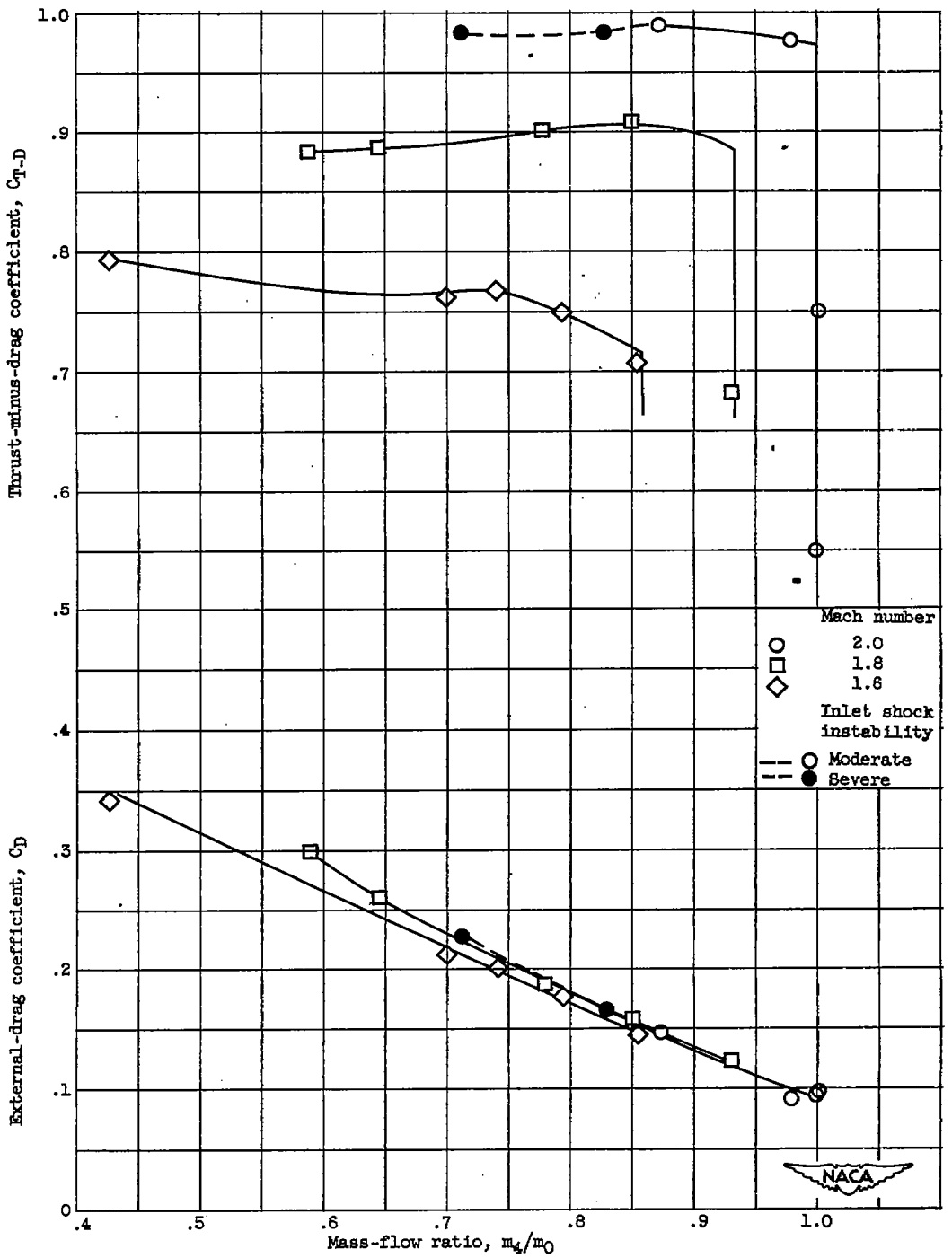

(b) Force coefficients.

Figure 3. - Concluded. Variation of inlet characteristics with mass-flow ratio for range of Mach numbers. Inlet A at zero angle of attack.

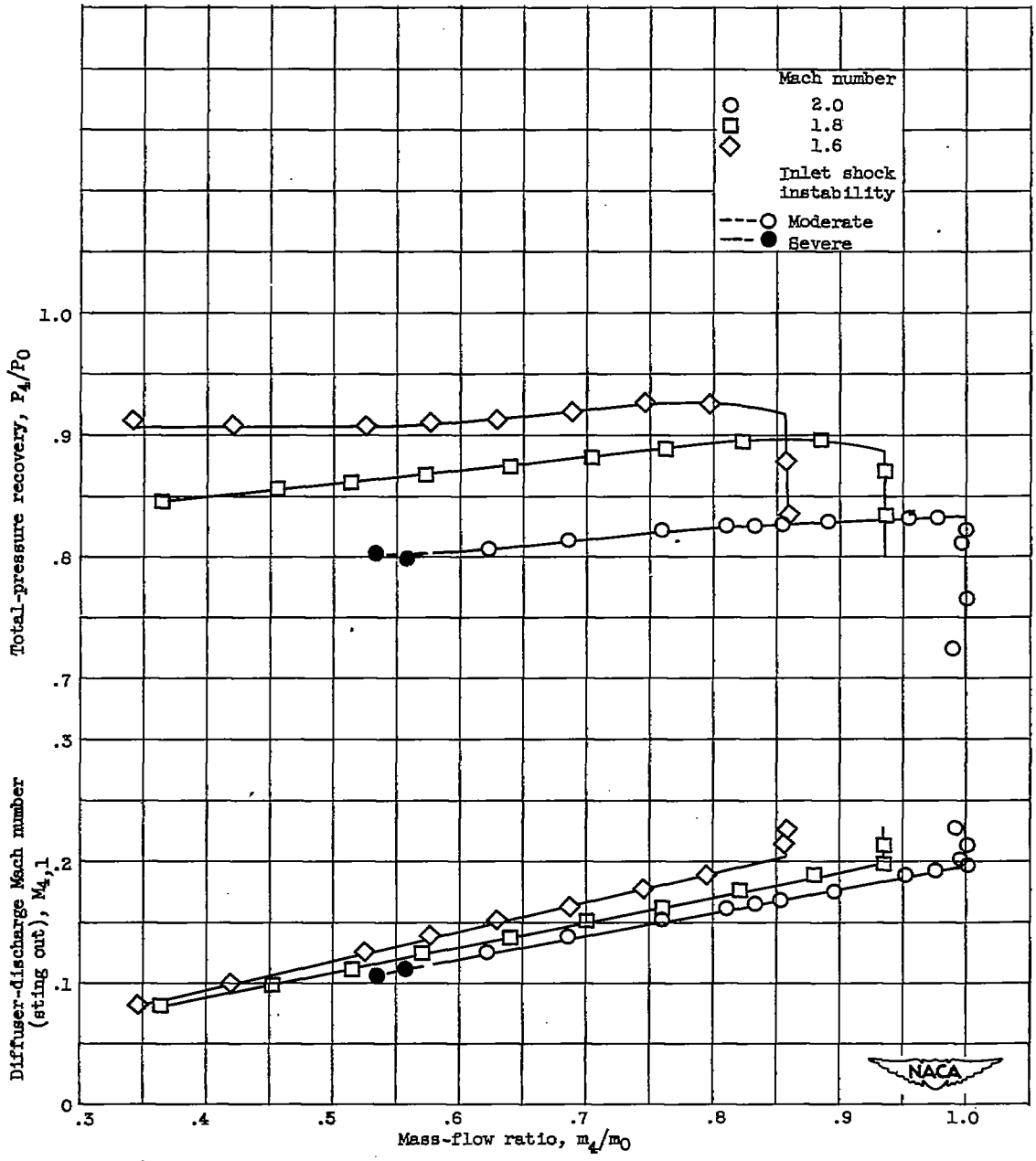

(a) Pressure recovery and diffuser-discharge Mach number characteristics.

Figure 4. - Variation of inlet characteristics with mass-flow ratio for a range of Mach numbers. Inlet B at zero angle of attack.

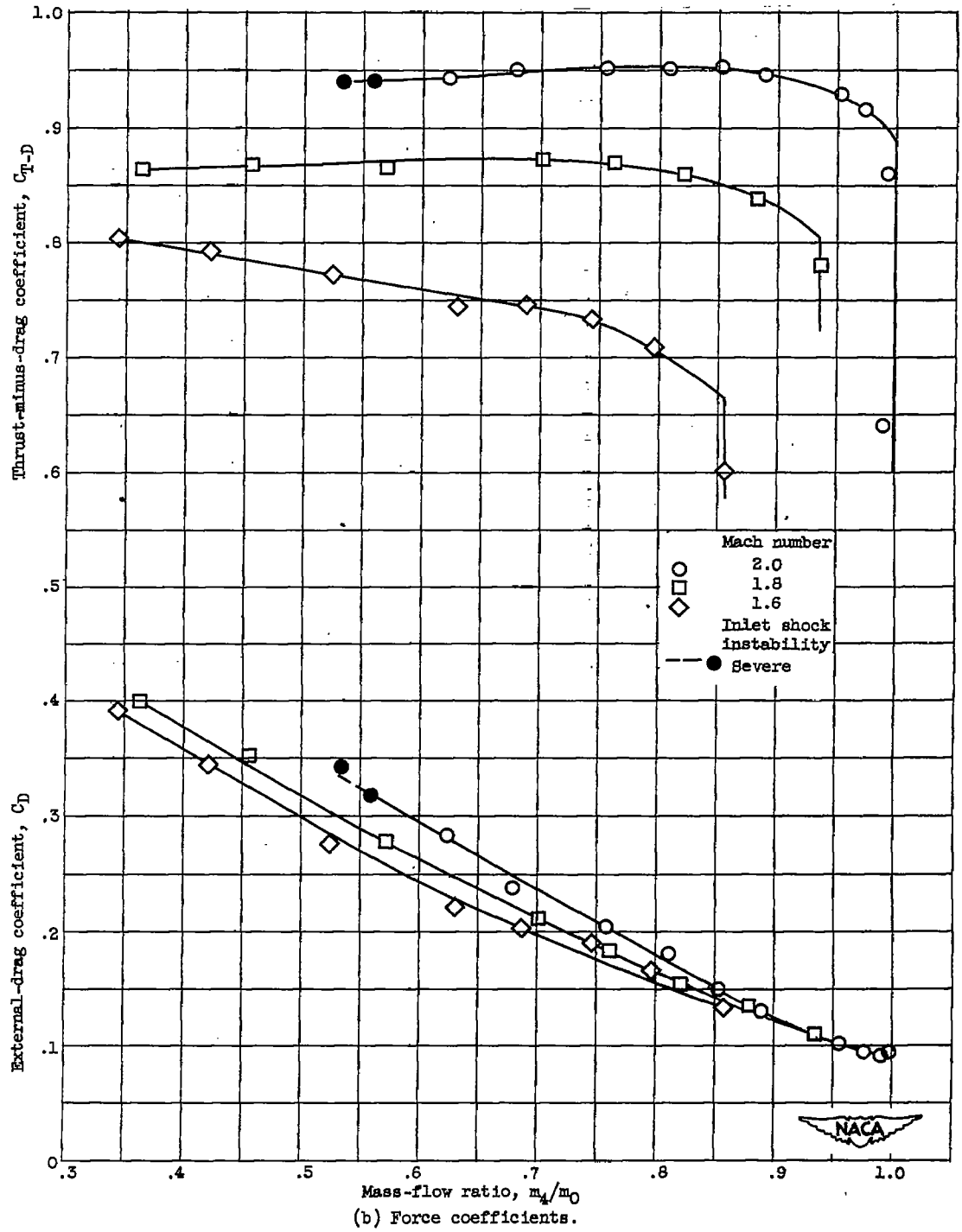

(b) Force coefficients.

Figure 4. - Concluded. Variation of inlet characteristics with mass-flow ratio for a range of Mach numbers. Inlet B at zero angle of attack.

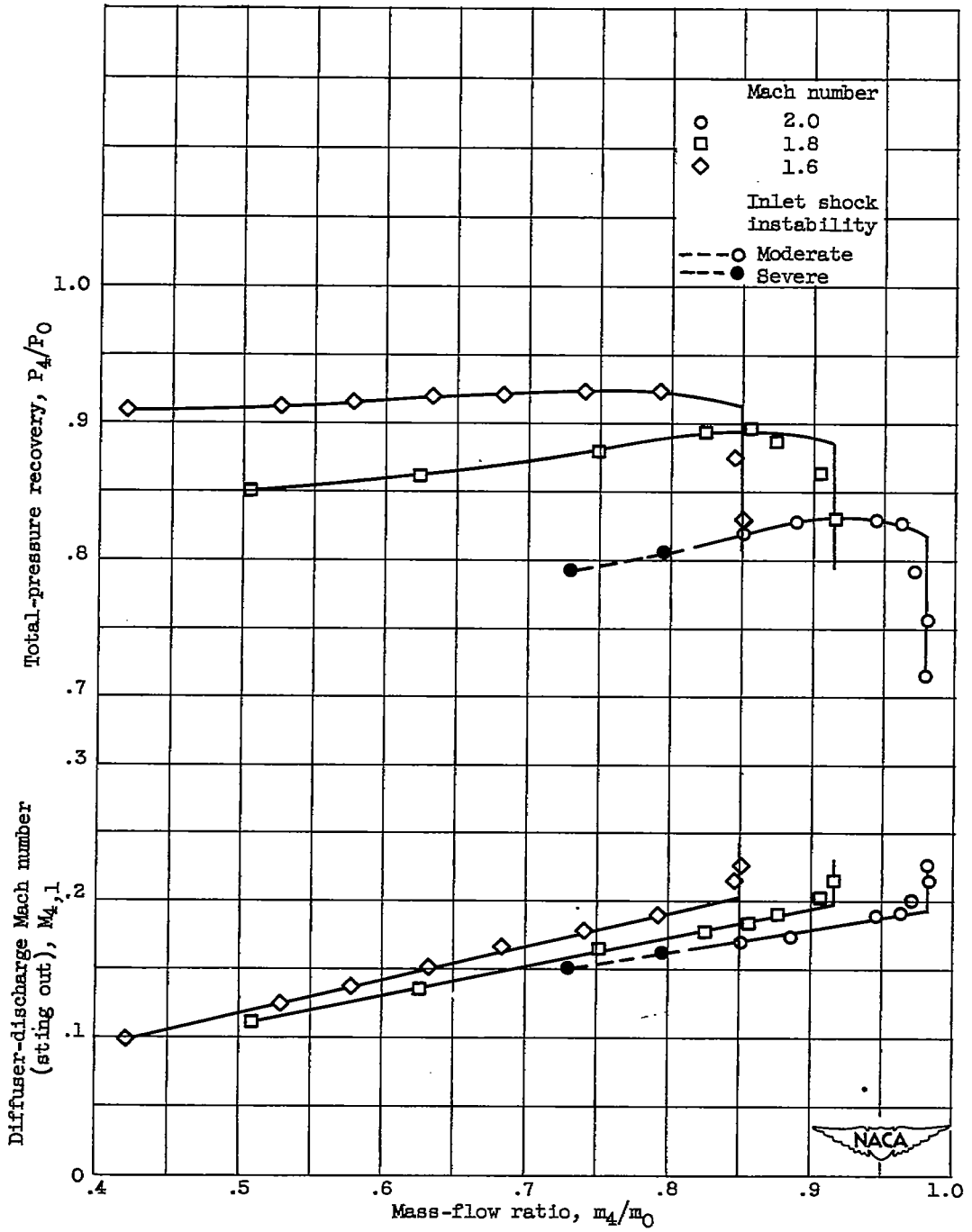

(a) Pressure-recovery and diffuser-discharge Mach number characteristics.

Figure 5. - Variation of inlet characteristics with mass-flow ratio for a range of Mach numbers. Inlet B at nominal angle of attack, 6°.

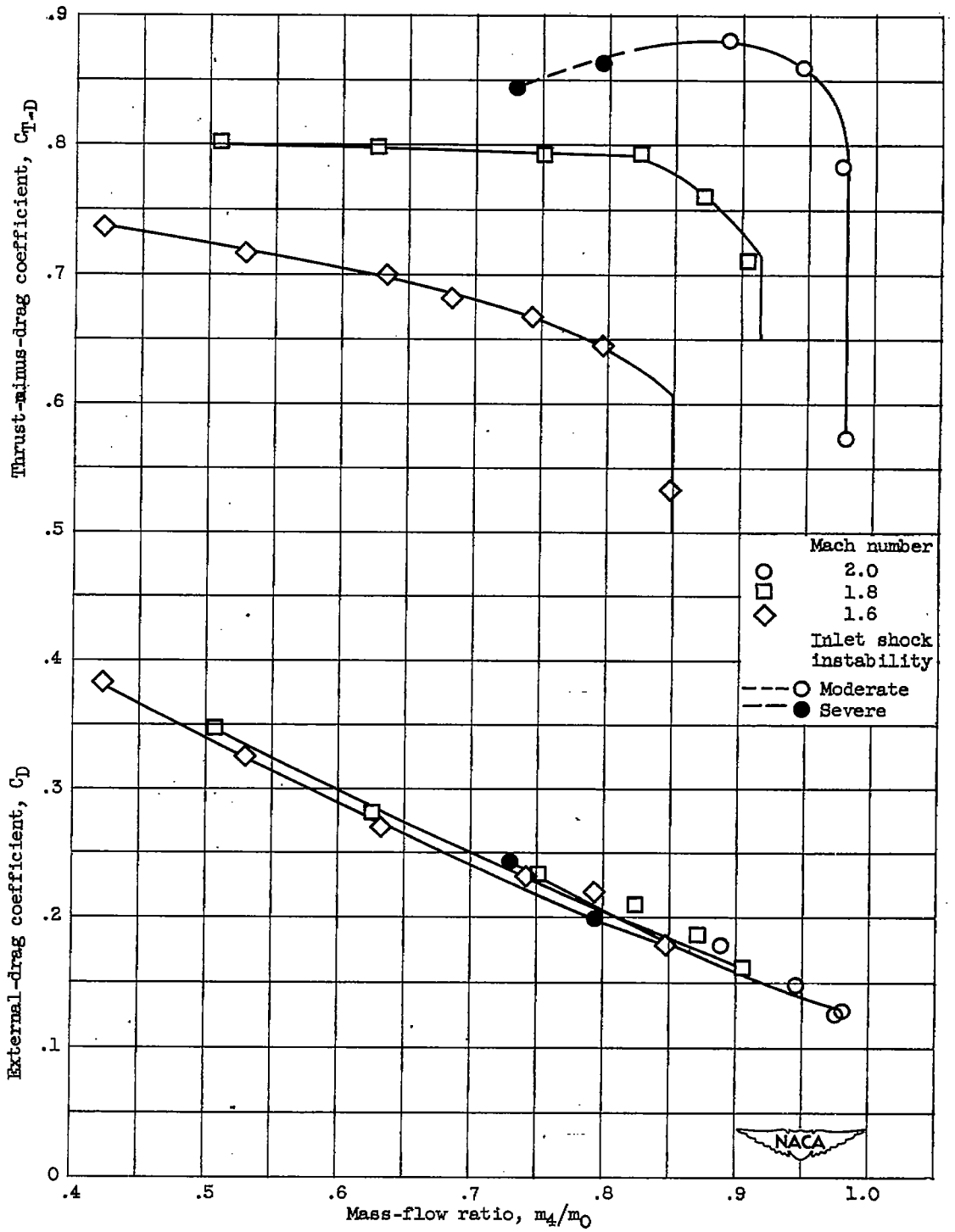

(b) Force coefficients.

Figure 5. - Concluded. Variation of inlet characteristics with mass-flow ratio for a range of Mach numbers. Inlet B at nominal angle of attack, 6°.

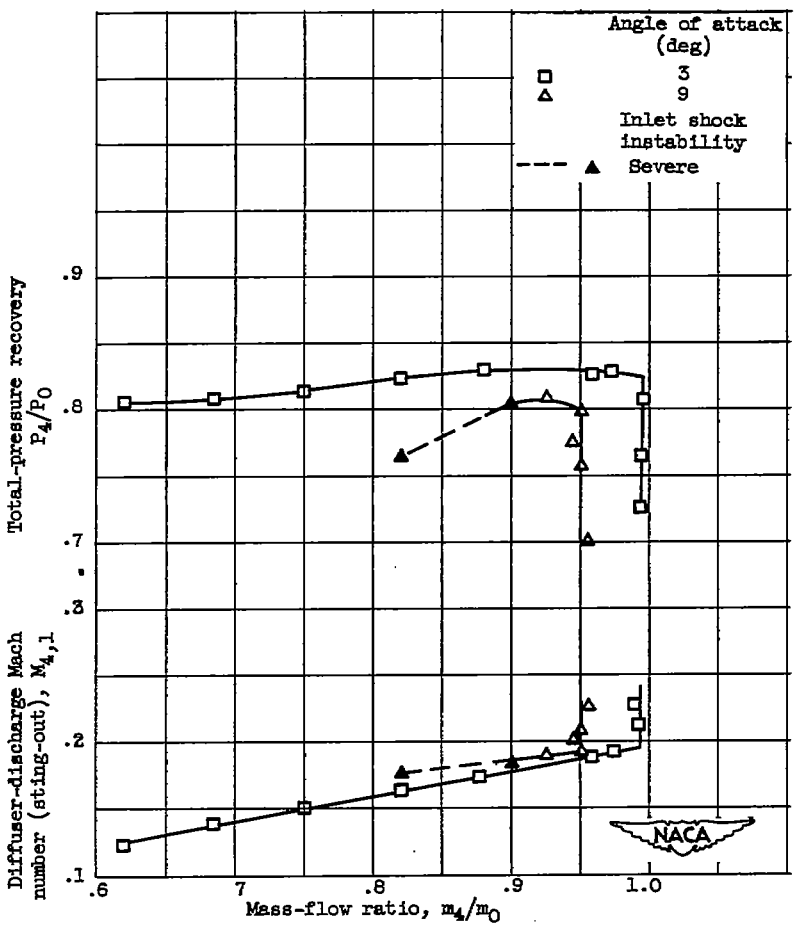

(a) Pressure-recovery and diffuser-discharge Mach number characteristics.

Figure 6. - Variation of inlet characteristics with mass-flow ratio for a Mach number of 2.0. Inlet B at nominal angles of attack, 3° and 9°.

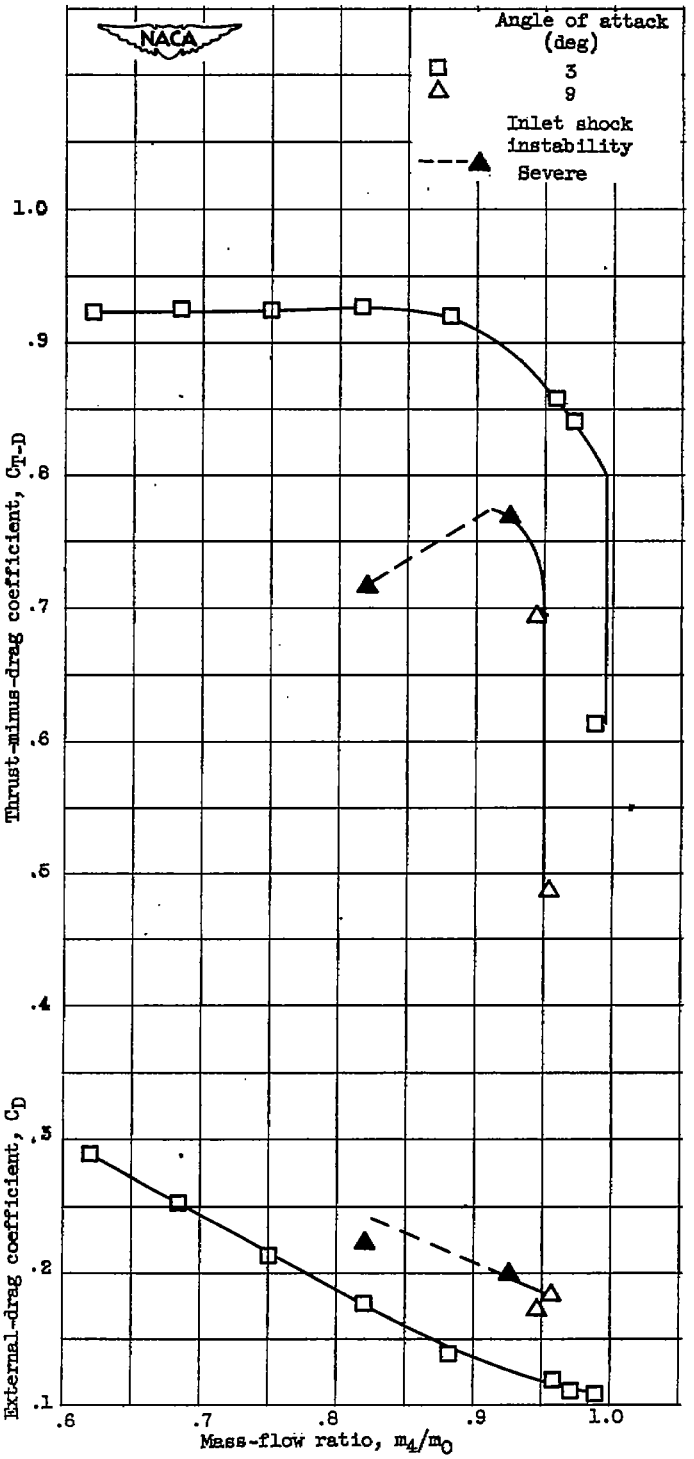

(b) Force coefficients.

Figure 6. - Concluded. Variation of inlet characteristics with mass-flow ratio for a Mach number of 2.0. Inlet B at nominal angles of attack, 3° and 9°.

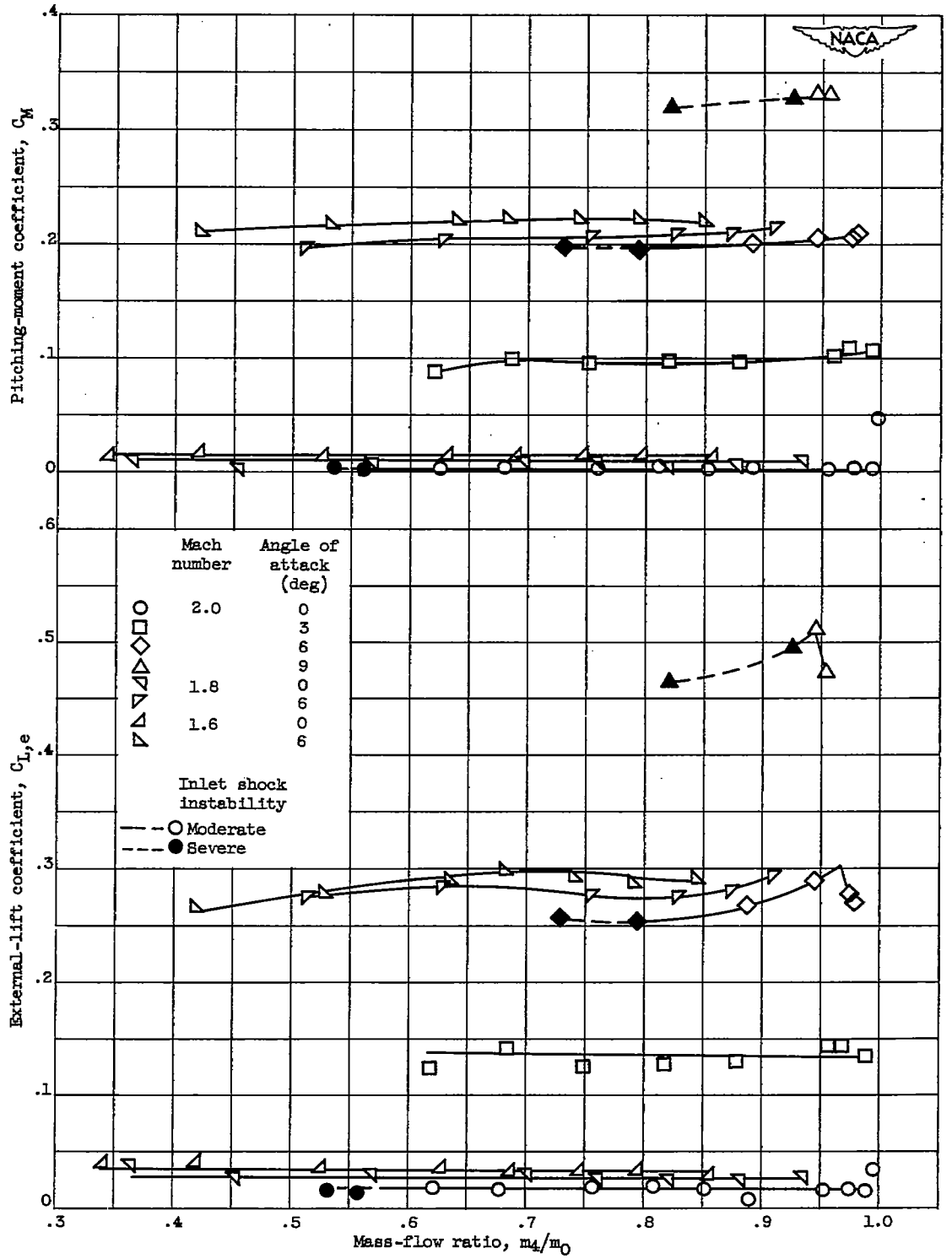

Figure 7. - Variation of lift and pitching-moment coefficients with mass-flow ratio for a range of Mach numbers. Inlet B at nominal angles of attack, 0°, 3°, 6°, and 9°.

NACA-Langley - 11-19-52 - 400